Optimizing the productivity in a chemostat model of plasmid-bearing plasmid-free competition: the case of general uptake functions*

NELI S. DIMITROVA

Institute of Mathematics and Informatics
Bulgarian Academy of Sciences
Acad. G. Bonchev Str. Bl. 8, 1113 Sofia, Bulgaria
nelid@math.bas.bg

Abstract: The paper investigates a dynamical model of plasmid-bearing, plasmid-free competition in the chemostat with general specific growth rates. Based on a feedback control, global stabilization of the dynamics towards a practically important coexistence equilibrium point is achieved. The latter result is used to optimize the productivity of the chemostat. Results from computer simulation are reported to illustrate the theoretical studies.

Key-Words: chemostat model, plasmid-bearing plasmid-free competition, feedback control, global stability, extremum seeking

1 Introduction

Genetically modified organisms are recently widely used for laboratory production of substances in biotechnological and pharmaceutical industry. The genetic modification is typically carried out by insertion of a DNA molecule into the cell in the form of a plasmid. These plasmid-bearing (parental) organisms are then growing in the chemostat. During the growth process the parental cells may lose the plasmid and revert to plasmid-free cells or cells that contain even modified plasmids. In most cases these revertant cells do not produce the desired product. The process is irreversible: if a cell has lost the plasmid, it is not possible to acquire it again. Examples reporting on this kind of instability for recombinant cell strains like *Escherichia coli, Bacillus subtilis, Saccharomyces cerevisiae* etc. can be found e. g. in [16], [24], [27] and the references therein. In large-scale production of recombinant DNA products the instability of the plasmid cell population is a major problem due to the great importance concerning the efficiency of the production processes, especially when the product is related to drug production for human use, quality of life and ecology, cf. [15], [18], [28].

The reason for plasmid instability during prolonged cultivation is not completely understood by theoretical biologists even at present time. The instability may be caused e. g. by the growth disadvantage of the parental cells in comparison with their plasmid-free variants: it has been experimentally validated that the plasmid-bearing cells have at least for some substrate concentrations a lower maximum specific growth rate than the plasmid-free counterparts (cf. [12], [14] and the references therein).

Lot of mathematical models are known in the literature to describe the dynamics of recombinant DNA in continuous culture [7], [16], [24], [30]. The models differ in their complexity but most of them describe the biological system in terms of competition between plasmid-bearing and plasmid-free (plasmid-modified) cells in the chemostat. The main goal in studying the mathematical models is to establish conditions for global asymptotic stability of the system and for persistence of the plasmid-bearing organism, cf. [6], [13], [27]. A useful approach for stabilization of highly unstable processes is based on applying different type of control strategies, cf. [3], [11], [20], [22], [23], [25] and the references therein. Among them feedback control is also a widely used technique for global stabilization [6], [9]. Feedback control, especially when it provides extra degrees of freedom, can also be applied to optimize the performance and the effectiveness of the chemostat, cf. [9], [10], [21].

In this paper we investigate the well known Levin-Stewart model [7], describing plasmid-bearing plasmid-free competition in the chemostat. The next Section 2 gives a short overview about ex-

*This work has been partially supported by the Sofia University "St Kl. Ohridski" under contract No. 109/19.04.2013.

istence, local stability/instability and bifurcations of the equilibrium points of the model. The new results in the paper are given in the following two sections. Section 3 is devoted to feedback control of the chemostat model; there we generalize the feedback law from [6], [8] to the case of general specific growth rate functions. Section 4 describes a numerical iterative algorithm for optimizing the productivity of the chemostat. Numerical results from computer simulations are also presented throughout the paper.

2 Preliminary results: equilibrium points, stability and bifurcations

We consider the classical mathematical model proposed in [7] which is probably the most widely studied model in the literature, see e. g. [1], [2], [6], [13], [17], [27]. The model is described by the following nonlinear ordinary differential equations

$$\begin{aligned} \dot{s} &= u(s^0 - s) - x_1\mu_1(s) - x_2\mu_2(s) \\ \dot{x}_1 &= x_1\left((1-q)\mu_1(s) - u\right) \\ \dot{x}_2 &= x_2(\mu_2(s) - u) + qx_1\mu_1(s), \end{aligned} \tag{1}$$

where $s(t)$, $x_1(t)$ and $x_2(t)$ are concentrations of substrate, plasmid-bearing organism and plasmid-free organism respectively, s^0 is the input substrate concentration, u is the dilution rate in the chemostat, $\mu_i(s)$, $i = 1, 2$, are the specific growth rates (uptake functions) of plasmid-bearing and plasmid-free organism respectively, q is a constant, presenting the probability of plasmid loss, $0 < q < 1$.

It is assumed that $\mu_i(s)$, $i = 1, 2$, are continuously differentiable and bounded, with $\mu_i(0) = 0$, $\mu_i(s) > 0$ for all $s > 0$.

It is not difficult to see that the solutions of (1) satisfy the following properties:

Theorem 1 (cf. [6], [13]).
(a) All solutions of (1) are nonnegative and bounded and thus exist for all $t \in [0, +\infty)$; moreover, $\lim_{t\to\infty}(s(t) + x_1(t) + x_2(t)) = s^0$.
(b) $\limsup_{t\to\infty} s(t) \le s^0$. □

The last property (b) allows us to consider only values of the substrate concentration s, such that $s \le s^0$.

In general, the number of the equilibrium points of (1) depends on the shape of the uptake functions as well as on the values of u and q.

The equilibrium points (of the form (s, x_1, x_2)) of the model are the following:

$E_0 = (s^0,\ 0,\ 0)$ always exists and is called the wash-out steady state;

$E_2 = (\alpha_2, 0, s^0 - \alpha_2)$, $F_2 = (\beta_2, 0, s^0 - \beta_2)$, where α_2 and β_2 solve the equation $\mu_2(s) = u$;

$E^e = (\alpha_1, x_1^e, x_2^e)$, $F^e = (\beta_1, \bar{x}_1^e, \bar{x}_2^e)$, where α_1 and β_1 solve $(1-q)\mu_1(s) = u$ and

$$\begin{aligned} x_1^e &= \frac{(s^0 - \alpha_1)(u - \mu_2(\alpha_1))}{\mu_1(\alpha_1) - \mu_2(\alpha_1)}, \\ x_2^e &= \frac{(s^0 - \alpha_1)q\mu_1(\alpha_1)}{\mu_1(\alpha_1) - \mu_2(\alpha_1)}; \\ \bar{x}_1^e &= \frac{(s^0 - \beta_1)(u - \mu_2(\beta_1))}{\mu_1(\beta_1) - \mu_2(\beta_1)}, \\ \bar{x}_2^e &= \frac{(s^0 - \beta_1)q\mu_1(\beta_1)}{\mu_1(\beta_1) - \mu_2(\beta_1)}. \end{aligned}$$

The equilibrium F_2 does not exist if $\mu_2(s)$ is monotone increasing (like the Monod law); also if $\mu_1(s)$ is monotone increasing then F^e does not exist. It follows from the analytical expressions of x_i^e and $\bar{x}_i^e$, $i = 1, 2$, that E^e respectively F^e exists if $\mu_2(\alpha_1) < u$ respectively $\mu_2(\beta_1) < u$ holds true. The latter inequalities imply $\mu_2(\alpha_1) < \mu_1(\alpha_1)$ and $\mu_2(\beta_1) < \mu_1(\beta_1)$ respectively. There is no equilibrium point corresponding to plasmid-bearing organism only (with $x_1 > 0$) and no plasmid-free organism (with $x_2 = 0$). This means that the chemostat can be operated only at a state where both populations are present [27].

Figures 1 and 2 visualize some particular cases of mutual disposition of inhibited (like the Haldane law [26]) uptake functions, as well as values of u such that the equilibrium points may or may not exist.

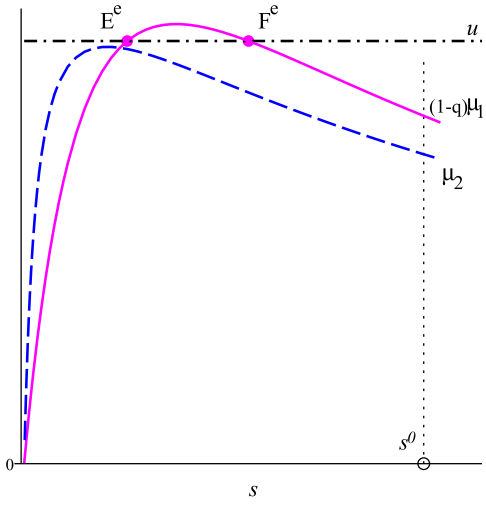

Figure 1. The equilibrium points E^e and F^e do exist

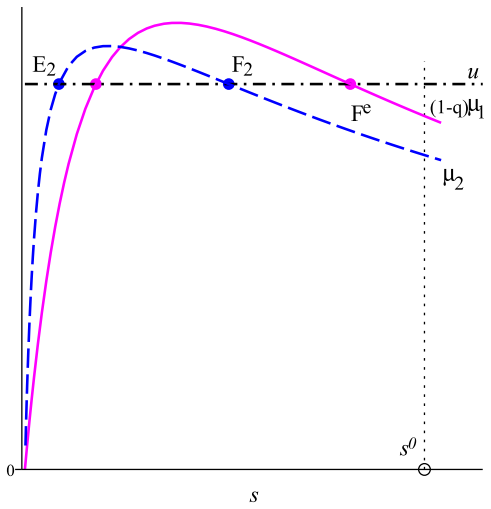

Figure 2. The equilibrium F^e does exist, E^e does not exist

Stability analysis of the equilibrium points is presented by many authors. Stephanopoulos and Lapidos [27] are probably the first who carried out detailed local stability analysis of the steady states considering Monod and Haldane kinetics for the specific growth rates of the organisms. The authors also reached to the conclusion that both organisms can survive if there exist ranges of substrate such that the plasmid-bearing cells have specific growth rate which is larger than the specific growth rate of the plasmid-free cells; in this case we say that the plasmid-bearing organism is a superior competitor in the chemostat.

Global asymptotic stability of the equilibrium points is established in [13] under the assumption that the uptake functions are monotone increasing for substrate concentrations $s \in [0, s^0]$. Later Luo and Hsu [17] extended the global asymptotic stability analysis in cases when (i) one of the uptake functions exhibits inhibition and the other is uninhibited, (ii) the specific growth rates of both populations are inhibited.

Figures 3 and 4 demonstrate the stability type of equilibrium points in some particular cases of shapes and mutual disposition of $(1-q)\mu_1(s)$ and $\mu_2(s)$. Depending on the values of u (on the vertical axis) only the locally stable equilibrium points are marked (on the right-hand side of each plot) in the corresponding regions of u. For example, see Figure 3, first plot, if u is high, $u > u_1$, then the wash-out steady state E_0 is the unique globally asymptotically stable equilibrium. If $u_1 < u < u_2$, then E_0 and E_2 are locally asymptotically stable; if $u < u_2$, then E_2 is the locally asymptotically stable equilibrium. The second plot in Figure 3 shows also a region for u where E_0, E_2 and E^e can be locally stable. It is worth to mention, that F^e is always unstable (saddle point) if it exists.

Bifurcations of the steady states with respect to the parameter u are established in details in [1], [2]. Bifurcations may occur for example at the threshold values $u = u_1$, $u = u_2$, see Figures 3 and 4. There exist also Hopf bifurcation points, denoted by solid circles in the plots.

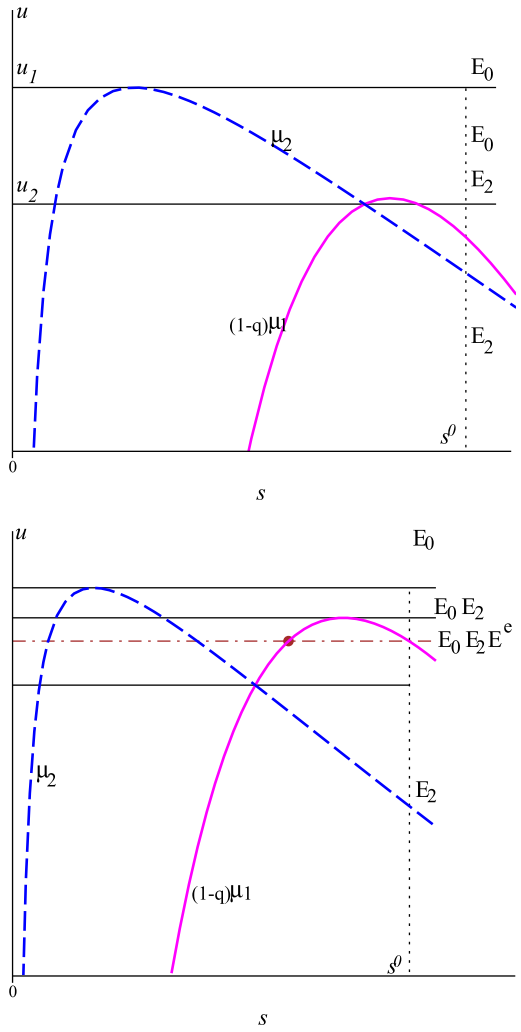

Figure 3. Locally stable equilibria are displayed; solid circle – Hopf bifurcation at E^e

Locating Hopf bifurcations is of great importance in biological systems. This is due to the fact that existence of limit cycles is very often a route of chaotic behaviour in dynamical models [19]. In [1], [2] the authors give a condition for the existence of a Hopf bifurcation point, namely: the model (1) can predict a Hopf point if the inequalities $\frac{d}{ds}\mu_1(s) > 0$ and $\frac{d}{ds}\mu_2(s) < 0$ at that point are simultaneously satisfied. Further, considering the Monod and the Haldane law as particular examples of uninhibited and inhibited specific growth rates, the authors determine a large number of regions in the parame-

ter space of the model (including the kinetic parameters in the uptake functions) where a variety of one-parameter local bifurcations (saddle-node, transcritical, Hopf bifurcations) can occur.

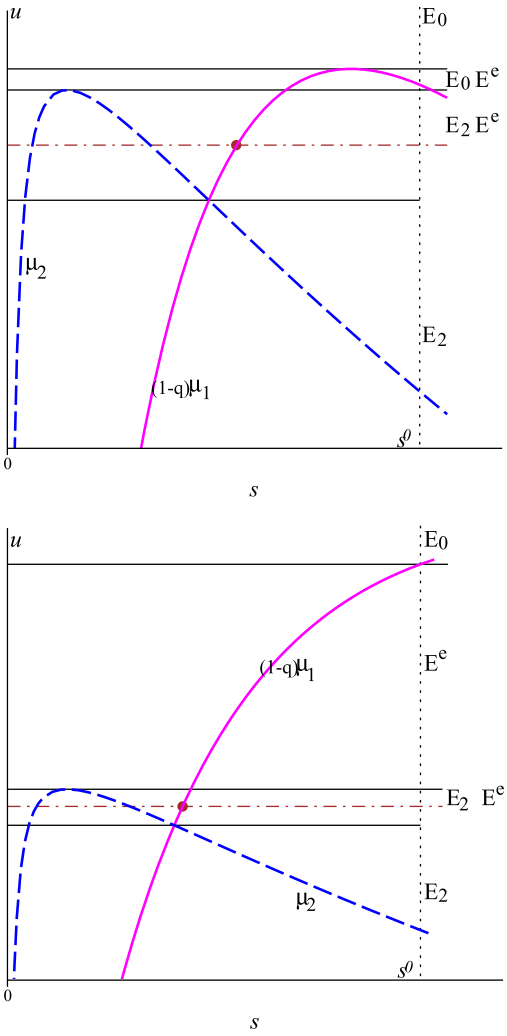

Figure 4. Locally stable equilibria are displayed; solid circle – Hopf bifurcation at E^e

3 Feedback control: general uptake functions

As mentioned above, it is not possible to achieve total efficiency of the chemostat by excluding the plasmid-free organisms [6], [13]. The best that can be done is to operate the chemostat in such a way, that both populations survive. This is possible by implementing the dilution rate u as a feedback law, depending on the system states, i. e. $u = u(s, x_1, x_2)$. Such a feedback is proposed in [6]. Thereby global stabilization of the model (1) and persistence of the plasmid-bearing organisms are proved in the case when the uptake functions satisfy the following conditions:

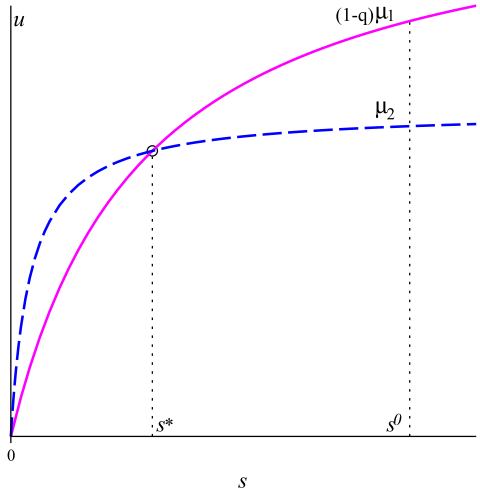

Figure 5. Monotone uptake functions

(a_1) $\mu_i(s)$, $i = 1, 2$, are monotone increasing, the graphs of $(1-q)\mu_1(s)$ and $\mu_2(s)$ intersect once at a point $s^* \in (0, s^0)$, i. e. $(1-q)\mu_1(s^*) = \mu_2(s^*) = u^*$;

(a_2) $(1-q)\mu_1(s) < \mu_2(s)$ for $s \in (0, s^*)$ and $(1-q)\mu_1(s) > \mu_2(s)$ for $s > s^*$.

Condition (a_2) means that for high substrate concentration ($s > s^*$) the plasmid-bearing organism is a superior competitor, while for low levels of s, $s < s^*$, the plasmid-free organism is superior, see Figure 5. Practical experiments show [27] that when the plasmid-bearing organism is superior, then coexistence of both organisms is possible.

We formulate the main result of [6] in the next theorem.

Theorem 2 [6]. Let the uptake functions μ_1 and μ_2 satisfy assumptions (a_1) and (a_2). Further for any $\epsilon \in (0, u^*)$ and $k > k^*$ with $k^* = \dfrac{u^* - \epsilon}{s^0 - s^*}$ define the following feedback

$$u(x_1, x_2) = k(x_1 + x_2) + \epsilon. \qquad (2)$$

Then there exists an equilibrium point $P = (s^p, x_1^p, x_2^p) > 0$ which is globally asymptotically stable for the closed-loop system (i. e. the system obtained from (1) by substituting u by the feedback $u(x_1, x_2)$ form (2)) with respect to initial conditions $s(0) \geq 0$, $x_1(0) > 0$, $x_2(0)) > 0$. □

In this section we shall generalize Theorem 2 for the case of nonmonotone uptake functions.

Denote by s_1^* and s_2^*, $s_1^* < s_2^*$, the crossing points (if exist) of the graphs of $(1-q)\mu_1(s)$ and $\mu_2(s)$; these points satisfy the equality

$$(1-q)\mu_1(s) = \mu_2(s), \quad s \in (0, s^0]. \qquad (3)$$

Let us mention that according to our assumption, $s = 0$ is always a solution of (3).

Figure 6 visualizes two different situations of shape and mutual disposition of inhibited uptake functions. There exist at most two crossing points s_1^* and s_2^* (despite $s = 0$) between the graphs of $(1-q)\mu_1(s)$ and $\mu_2(s)$. In the first plot the plasmid-bearing organism is a superior competitor for $s \in (s_1^*,\ s^0)$. In the second plot the plasmid-bearing organism is superior for $s \in (s_1^*,\ s_2^*)$.

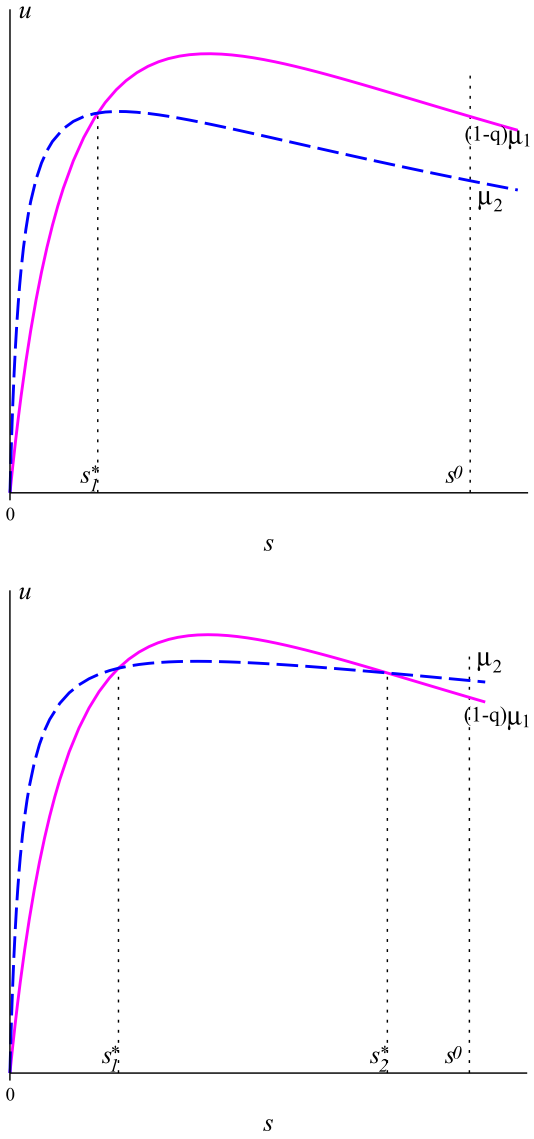

Figure 6. Inhibited uptake functions

Define further the values

$$\begin{aligned} u_1^* &= \mu_2(s_1^*), \\ u_2^* &= \begin{cases} \mu_2(s_2^*) & \text{if } s_2^* < s^0, \\ \mu_2(s^0) & \text{if } s_2^* \geq s^0; \end{cases} \\ u^* &= \min\{u_1^*,\ u_2^*\} \end{aligned} \tag{4}$$

and the constants

$$m = \min\left\{\min_{[0,s^0]} \frac{d}{ds}\mu_1(s),\ \min_{[0,s^0]} \frac{d}{ds}\mu_2(s)\right\} \tag{5}$$

$$\delta = \begin{cases} u^* + (s^0 - s_1^*)\cdot m & \text{if } m < 0, \\ u^* & \text{if } m \geq 0. \end{cases} \tag{6}$$

Assume that $\delta > 0$. Let $d \in [0, \delta)$ and define the feedback

$$\kappa(x_1, x_2) = k\,(x_1 + x_2) + d, \tag{7}$$

where the constant $k > 0$ is chosen according to the following scheme:

---

k-determining scheme

I. If $0 < s_1^* < s^0 \leq s_2^*$, define
$k_1 = \dfrac{u_1^* - d}{s^0 - s_1^*}$;

Ia. If $(1-q)\mu_1(s) > \mu_2(s)$ for $s \in (0,\ s_1^*)$ then choose $k < k_1$;

Ib. If $(1-q)\mu_1(s) > \mu_2(s)$ for $s \in (s_1^*,\ s^0)$ then choose $k > k_1$;

II. If $0 < s_1^* < s_2^* < s^0$, define
$k_1 = \dfrac{u_1^* - d}{s^0 - s_1^*}$, $k_2 = \dfrac{u_2^* - d}{s^0 - s_2^*}$;

IIa. If $(1-q)\mu_1(s) > \mu_2(s)$ for $s \in (s_1^*,\ s_2^*)$ then choose $k \in (k_1, k_2)$;

IIb. If $(1-q)\mu_1(s) > \mu_2(s)$ for $s \in (0,\ s_1^*) \cup (s_2^*,\ s^0]$ then choose

$$k \begin{cases} < k_1, & \text{if} \quad s \in (0, s_1^*) \\ > k_2, & \text{if} \quad s \in (s_2^*, s^0). \end{cases}$$

Remark 1. The inequality $m > 0$ in (6) means that $\mu_1(s)$ and $\mu_2(s)$ are monotone increasing (uninhibited) functions in $[0, s^0]$.

Remark 2. The assumption $\delta > 0$ seems to be rather restrictive but it is not. If $\mu_1(s)$ and $\mu_2(s)$ are monotone increasing then $\delta > 0$ is always satisfied. In the case when at least one of $\mu_1(s)$, $\mu_2(s)$ is inhibited, this assumption is satisfied for all practically known specific growth rates if the input substrate concentration s^0 is not too large (which is also practically the case).

Denote by Σ the closed-loop system, which is obtained from (1) by substituting u by the feedback $\kappa(x_1, x_2)$ from (7):

$$\begin{aligned} \dot{s} &= \kappa(x_1, x_2)\,(s^0 - s) - x_1\mu_1(s) - x_2\mu_2(s) \\ \dot{x}_1 &= x_1\,((1-q)\mu_1(s) - \kappa(x_1, x_2)) \\ \dot{x}_2 &= x_2\,(\mu_2(s) - \kappa(x_1, x_2)) + q x_1 \mu_1(s). \end{aligned} \tag{8}$$

Theorem 3. Let the feedback $\kappa(x_1, x_2)$ be defined according to (7) with all constants determined by (4)–(6) and the k-determining scheme. Then there exists an equilibrium point $E_c = (s^c, x_1^c, x_2^c) > 0$ which is globally asymptotically stable for the closed-loop system Σ with respect to initial conditions $s(0) \geq 0$, $x_1(0) > 0$, $x_2(0) > 0$.

Proof. The proof is similar to that of Theorem 2 (see [6]). We present below the main steps of the proof for the case IIa; the other cases are treated similarly. Let $(s(t), x_1(t), x_2(t))$ be any solution of (8) starting from $(s(0), x_1(0), x_2(0))$. According to Theorem 1(a), $\lim_{t\to\infty}(s(t) + x_1(t) + x_2(t)) = s^0$ holds true. This means that the ω-limit set of every solution belongs to the set

$$\Omega^r = \left\{(s, x_1, x_2) : \; s + x_1 + x_2 = s^0\right\},$$

i. e. Ω^r is positively invariant for Σ. On Ω^r, the feedback can be presented in the form

$$\kappa(x_1, x_2) = \kappa(s) = k(s^0 - s) + d.$$

Geometrically, the coefficient k in $\kappa(s)$ represents the slope of a straight line, which is shown in Figure 7 as solid line, together with the boundary lines (the dash-dot lines) with slopes k_1 and k_2.

The system Σ possesses three equilibrium points:

$E_0 = (s^0, 0, 0)$;

$E_2 = (\alpha_2^c, 0, s^0 - \alpha_2^c)$, where α_2^c is the unique solution of $\mu_2(s) = k(s^0 - s) + d$;

$E_c = (s^c, x_1^c, x_2^c)$, where s^c is the unique solution of $(1-q)\mu_1(s) = k(s^0 - s) + d$ and

$$\begin{aligned} x_1^c &= \frac{(s^0 - s^c)((1-q)\mu_1(s^c) - \mu_2(s^c))}{\mu_1(s^c) - \mu_2(s^c)}, \\ x_2^c &= s^0 - s^c - x_1^c. \end{aligned}$$

Consider the restriction Σ^r of Σ on Ω^r by replacing s by $s^0 - x_1 - x_2$:

$$\begin{aligned} \dot{x}_1 &= x_1\left((1-q)\mu_1(s^0 - x_1 - x_2) - \kappa(x_1, x_2)\right) \\ \dot{x}_2 &= x_2\left(\mu_2(s^0 - x_1 - x_2) - \kappa(x_1, x_2)\right) \\ &\quad + qx_1\mu_1(s^0 - x_1 - x_2) \end{aligned} \tag{9}$$

within $x_1(0) > 0$, $x_2(0) > 0$, $x_1(0) + x_2(0) \leq s^0$.

The equilibrium points of (9) are

$$E_0^r = (0, 0), \quad E_2^r = (0, s^0 - \alpha_2^c), \quad E_c^r = (x_1^c, x_2^c).$$

Denote the vector field in the right-hand side of (9) by $f(x_1, x_2)$. By calculating the Jacobian matrices of $f(x_1, x_2)$ at the three steady states E_0^r, E_2^r, E_c^r, it follows that

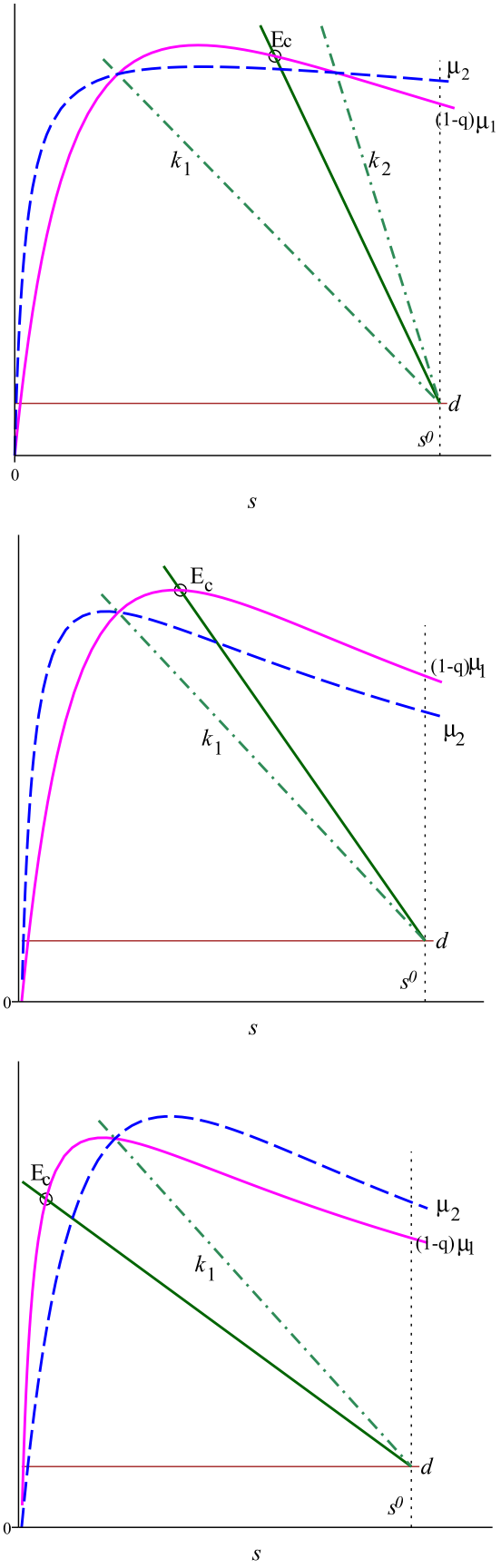

Figure 7. Graphical interpretation of the choice of k: $k_1 < k < k_2$ (first plot), $k > k_1$ (second plot), $k < k_1$ (third plot). The solid lines have a slope k

E_0^r is a repeller,
E_2^r is a saddle point (unstable),
E_c^r is locally asymptotically stable (attractor).

The Butler–McGehee theorem [26] implies that E_2^r cannot belong to the ω-limit set of solutions with positive initial conditions $x_i(0) > 0$, $i = 1, 2$. Further, the existence of nontrivial periodic solutions for Σ^r can also be excluded by means of the Dulac criterion [26]: the divergence of the vector field $\frac{1}{x_1 x_2} f(x_1, x_2)$ is equal to

$$\begin{aligned}\operatorname{div} \frac{1}{x_1 x_2} f(x_1, x_2) \\ = \; & -\frac{1}{x_2}\left(\frac{d\mu_1}{ds}(s^0 - x_1 - x_2) + k\right) \\ & -\frac{1}{x_1}\left(\frac{d\mu_2}{ds}(s^0 - x_1 - x_2) + k\right) \\ & -\frac{q\mu_1(s^0 - x_1 - x_2)}{x_2^2}.\end{aligned}$$

According to the choice of the constants m, δ, d and k, we have consecutively

$$\begin{aligned} & d < \delta = u^* + (s^0 - s_1^*)m \le u_1^* + (s^0 - s_1^*)m \\ & u_1^* - d > -(s^0 - s_1^*)m \\ & \frac{u_1^* - d}{s^0 - s_1^*} > -m \\ & k_1 + m > 0 \\ & k + m > k_1 + m > 0. \end{aligned}$$

The last inequality leads to $\frac{d}{ds}\mu_i(s^0 - x_1 - x_2) + k > 0$, $i = 1, 2$, thus

$$\operatorname{div} \frac{1}{x_1 x_2} f(x_1, x_2) < 0.$$

Using the Dulac criterion we obtain that there are no nontrivial periodic orbits around E_c^r. The Poincaré-Bendixon theorem [26] further implies that the equilibrium E_c^r is globally asymptotically stable for Σ^r. Finally, using an extension of LaSalle's invariance principle [4], we obtain that E_c is globally asymptotically stable equilibrium for Σ. □

Numerical simulation. To demonstrate the advantages of the feedback control, we consider a numerical example with two Haldane uptake functions

$$\begin{aligned}\mu_1(s) &= \frac{m_1 s}{a_1 + s + \gamma_1 s^2}, \\ \mu_2(s) &= \frac{m_2 s}{a_2 + s + \gamma_2 s^2},\end{aligned}$$

where

$$\begin{aligned} & m_1 = 1,\ a_1 = 1,\ \gamma_1 = 0.16, \\ & m_2 = 0.5,\ a_2 = 0.015,\ \gamma_2 = 0.04; \end{aligned}$$

The uptake functions are visualized in Figure 3, second plot.

Several trajectories of the open-loop system (1) in the (x_1, x_2)-plane are displayed in the first plot of Figure 8. Depending on the initial conditions, we observe the existence of a limit cycle (Hopf bifurcation) as well as of wash-out of the plasmid-bearing organisms in the first plot. The second plot shows the trajectories of the closed-loop system (8) with the same initial conditions; the parameter k in the feedback (7) is chosen in such a way that the global attractor E_c of (8) coincides with the Hopf bifurcation point of (1) (the solid circle in both plots).

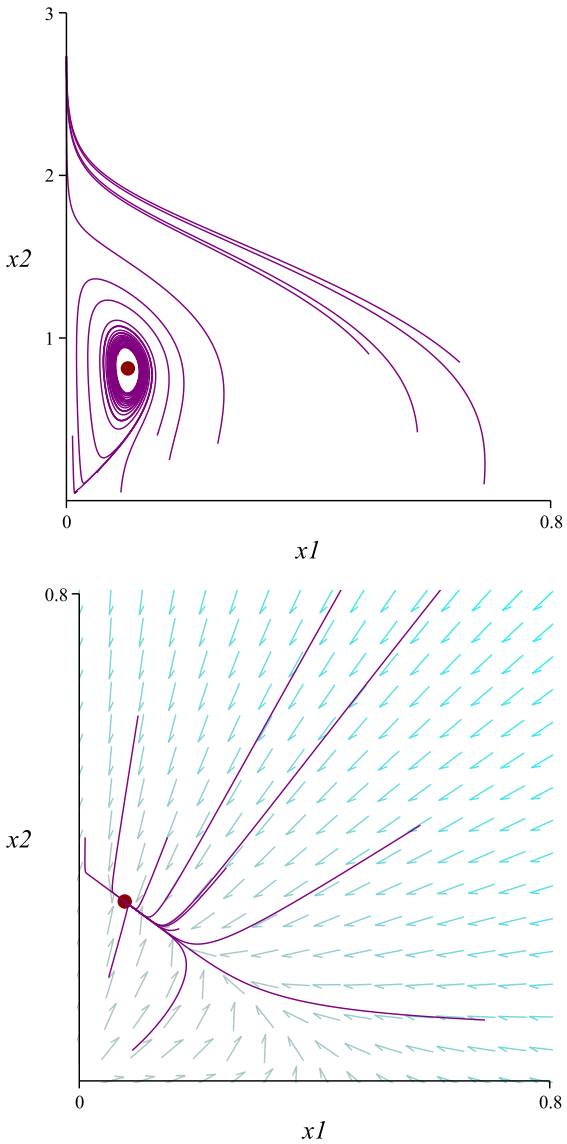

Figure 8. First plot: trajectories of the open-loop system; solid circle – Hopf bifurcation point. Second plot: trajectories of the closed-loop system; solid circle – the global attractor E_c

4 Model-based optimization of the chemostat dynamics

We have already seen that the chemostat can be operated only at a steady state, where both plasmid-bearing and plasmid-free organisms exist together. An open problem posed in [13] is whether it is possible to maximize the concentration of the plasmid-bearing organisms. Here we present a solution of this problem. We shall use the fact that E_c is globally asymptotically stable *for any choice of* k according to the above k-determining scheme. It is easy to see that the steady state component $x_1^c = x_1^c(k)$ of $E_c = E_c(k)$, considered as a function of the parameter k, possesses a maximum $x_{1,max}^c = x_1^c(k^m)$ at a unique (and unknown) value of $k = k^m$, independently on the shapes of the uptake functions, see the first plot in Figure 9.

To maximize the concentration $x_1(t)$ of the plasmid-bearing organisms in real time we shall use a model-based iterative extremum seeking algorithm.

Optimization via extremum (peek) seeking is another control approach extensively used in the last decade to optimize the productivity of a continuously stirred tank bioreactor. In the literature [5], [29], the extremum seeking approach is not model-based: the algorithm is usually presented in the form of a block-scheme to iteratively adjust the dilution rate directly in the bioreactor in order to steer the process to a point, where optimal value of the output is achieved. The main restriction in applying this model-free extremum seeking approach is that the dynamics should be open-loop stable; otherwise, a locally stabilizing controller is needed to stabilize the equilibrium points around the optimal operating point.

Our approach is different; we first stabilize globally the dynamical system via feedback control and then apply the extremum seeking method to drive the dynamics towards the desired state. The numerical extremum seeking algorithm was originally designed to solve an optimization problem for a two-dimensional bioreactor model [9] and further extended for models of wastewater treatment processes [10]. Here the algorithm is adapted and applied to this model.

The algorithm is executed in two main stages.

In the first stage, an interval $[K] = [K^-, K^+]$ is determined, such that $k^m \in [K]$; this is achieved by constructing in a proper way a sequence of points $k^{(0)}, k^{(1)}, \ldots, k^{(i)}, \ldots$, of the form $k^{(i)} = k^{(i-1)} + \sigma h$, $\sigma = \pm 1$, $h > 0$, such that for any $k^{(i)}$ there exists $x_1^c(k^{(i)})$, and $E_c(k^{(i)})$ is a globally stable equilibrium according to Theorem 3.

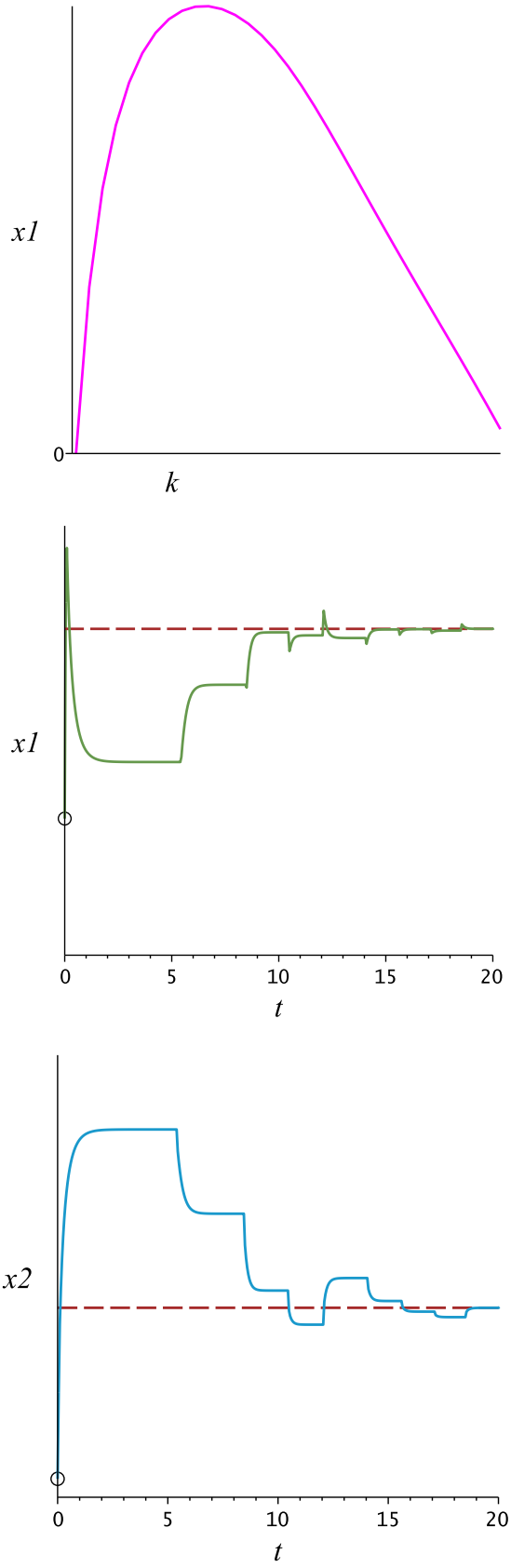

Figure 9. First plot: the steady state component $x_1^c = x_1^c(k)$ of the global attractor E_c. Second and third plot: time evolution of $x_1(t)$ and $x_2(t)$; the dashed lines pass through $x_{1,\max}^c = x_1^c(k^m)$ and $x_2^c(k^m)$ respectively

In the second stage the interval $[K]$ is refined by means of Fibonacci elimination techniques to obtain a subinterval $[K^m] = [K^{m-}, K^{m+}] \subset [K]$ such that $k^m \in [K^m]$ with $K^{m+} - K^{m-} \leq \varepsilon$, where $\varepsilon > 0$ is a user-defined tolerance.

The second and third plots in Figure 9 show results from numerical simulation within Haldane specific growth rates, visualized in the first plot of Figure 7. The "jumps" in the solutions correspond to the different choice of the constants $k^{(i)}$ in the extremum seeking algorithm

The extremum seeking algorithm is applicable to any uptake functions μ_1 and μ_2, exhibiting or not inhibition. The only information needed is about the existence of at least one crossing point $s_1^* < s^0$ such that the plasmid-bearing organism is a superior competitor for $s > s_1^*$ or $s < s_1^*$.

The algorithm can be implemented to work online.

5 Conclusion

The paper investigates the classical Levin-Stewart model for plasmid-bearing plasmid-free competition in the chemostat. The feedback control law, proposed in [6] for uninhibited specific growth rates of the organisms, is extended for the case of general uptake functions $\mu_1(s)$ and $\mu_2(s)$. The main difference is in the choice of the parameter k. The new feedback stabilizes globally the closed loop system towards an equilibrium point, where persistence of both organisms is enhanced in the chemostat. Using the freedom in choosing k an extremum seeking algorithm is applied to optimize the chemostat productivity. The theoretical results are illustrated on numerical examples.

References

[1] A. Ajbar, Classification of Static and Dynamic Behavior in Chemostat for Plasmid-bearing, Plasmid-free Mixed Recombinant Cultures, *Chem. Eng. Comm.*, No. 189, 2002, pp. 1130–1154.

[2] K. Alhumaizi, A. Alwan, A. Ajbar, Competition of Plasmid-bearing and Plasmid-free Organisms in a Chemostat: a Study of Bifurcation Phenomena, *Mathematical and Computer Modelling*, Vol. 44, 2006, pp. 342–367.

[3] M. Angelova, P. Melo-Pinto, T. Pencheva, Modified Simple Genetic Algorithms Improving Convergence Time for the Purposes of Fermentation Process Parameter Identification, *WSEAS Transaction on Systems*, Vol. 11, Issue 7, 2012, pp. 257–267.

[4] A. Arsie, Ch. Ebenbauer, Locating Omegalimit Sets Using Height Functions, *Journal of Differential Equations*, Vol. 248, No. 10, 2010, pp. 2458–2469.

[5] K. B. Ariyur, M. Ktstić, *Real-time optimization by extremum-seeking control*, John Wiley & Sons, Hoboken, New Jersey, 2003.

[6] P. De Leenheer, H. Smith, Feedback Control for Chemostat Models, *J. Math. Biol.*, No. 46, 2003, pp. 48–70.

[7] B. R. Levin, F. M. Stewart, The Population Biology of Bacterial Plasmids: a priori Conditions for the Existence of Mobilizable Nonconjugative Factors, *Genetics*, Vol. 94, No. 2, 1980, pp. 425–443.

[8] N. Dimitrova, Modeling the Production of Genetically Modified Organisms in the Chemostat, *Mathematica Balkanica, New Series*, Vol. 25, Fasc. 3, 2011, pp. 277–291.

[9] N. Dimitrova, M. Krastanov, Nonlinear Adaptive Control of a Model of an Uncertain Fermentation Process, *Int. Journ. of Robost and Nonlinear Control*, No. 20, 2010, pp. 1001–1009.

[10] N. Dimitrova, M. I. Krastanov, On the Asymptotic Stabilization of an Uncertain Bioprocess Model, In: I. Lirkov, S. Margenov, J. Wańsiewski (Eds.), Proc. LSSC'2011, Lecture Notes in Computer Sciences, Springer, 7116, 2012, pp. 115–122.

[11] N. S. Dimitrova, M. I. Krastanov, On the Asymptotic Stabilization of an Anaerobic Digestion Model with Unknown Kinetics, *WSEAS Transactions on Systems*, Vol. 11, Issue 7, 2012, pp. 244–255.

[12] V. Y. Ganusov, A. V. Brilkov, Estimating the Instability Parameters of Plasmid-Bearing Cells. I. Chemostat Culture, *J. Theor. Biol.*, Vol. 219, 2002, pp. 193–205.

[13] S.-B. Hsu, P. Waltman, G. S. Wolkowicz, Global Analysis of a Model of Plasmid-bearing, Plasmid-free Competition in a Chemostat, *J. Math. Biol.*, No. 32, 1994, pp. 731–742.

[14] T. Imanaka, S. Aiba, A Perspective on the Application of Genetic Engineering: Stability of Recombinant Plasmid, *Ann. N. Y. Acad. Sci.*, No. 369, 1981, pp. 1–14.

[15] P. Jirava, J. Mandys, M. Kasparova, J. Krupka, System Approach to Determinants of Quality of Life within a Region, *WSEAS Transaction on Systems*, Vol. 9, Issue

3, 2010, pp. 243–252.

[16] S. B. Lee, J. E. Bailey, Analysis of the Growth Rate Effects on Productivity of Recombinant *E. coli* Populations Using Molecular Mechanism Models, *Biotechnol. Bioeng.*, No. 26, 1984, pp. 66–73.

[17] T.-K. Luo, S.-B. Hsu, Global Analysis of a Model of Plasmid-bearing, Plasmid-free Competition in a Chemostat with Inhibition, *J. Math. Biol.*, No. 34, 1995, pp. 41–76.

[18] S. D. Mileva, S. I. Vassileva, Pl. Ts. Andreeva, Intelligent Systems and their Applications in Software Sensor Systems for Industrial Product Safety and Ecology, *Journal Ecology&Safety*, Vol. 2, 2008, pp. 519–530.

[19] L. Nechak, S. Berger, E. Aubry, Robust Analysis of Uncertain Dynamic Systems: Combination of the Centre Manifold and Polynomial Chaos theory, *WSEAS Transaction on Systems*, Vol. 9, Issue 4, 2010, pp. 386–395.

[20] F. Neri, Cooperative evolutive concept learning: an empirical study, *WSEAS Transaction on Information Science and Applications*, WSEAS Press (Wisconsin, USA), Vol. 2, Issue 5, 2005, pp. 559–563.

[21] P. C. Patic, L. Duta, Comparative Study Regarding the Optimization and Analysis of Automatic Systems using PID, LQR and PIMIMO, *WSEAS Transactions on Systems*, Vol. 9, No. 7, 2010, pp. 754–763.

[22] Kl. Röbenack, N. Dingeldey, Observer Based Current Estimation for Coupled Neurons, *WSEAS Transaction on Systems*, Vol. 11, Issue 7, 2012, pp. 268–281.

[23] D. F. Ryder, D. DiBiasio, An Operational Strategy for Unstable Recombinant DNA Cultures, *Biotechnol. Bioeng.*, Vol. 26, 1984, pp. 942–947.

[24] D. F. Ryder, D. DiBiasio, A Model for Growth of Saccharomyces cerevisiae Containing a Recombinant Plasmid in Selective Media, *Biotechnol. Bioeng.*, Vol. 29, No. 4, 1987, pp. 469–475.

[25] Ts. Slavov, O. Roeva, Application of Genetic Algorithm to Tuning a PID Controller for Glucose Concentration Control, *WSEAS Transaction on Systems*, Vol. 11, Issue 7, 2012, pp. 223–233.

[26] H. L. Smith, P. Waltman, *The Theory of the Chemostat. Dynamics of Microbial Competition*, Cambridge University Press, 1995.

[27] G. Stephanopoulos, G. R. Lapidus, Chemostat Dynamics of Plasmid-bearing, Plasmid-free Mixed Recombinant Cultures, *Chem. Eng. Sci.* No. 43, 1988, pp. 49–57.

[28] S. Vassileva, Advanced Fuzzy Modeling of Integrated Bio-Systems, *WSEAS Transaction on Systems*, Vol. 11, Issue 7, 2012, pp. 234–243.

[29] H.-H. Wang, M. Krstić, G. Bastin, Optimizing Bioreactors by Extremum Seeking, *Int. J. Adapt. Control Signal Process*, Vol. 13, 1999, pp. 651–669.

[30] J. Wu, H. Nie, G. S. K. Wolkowicz, The Effect of Inhibitor on the Plasmid-Bearing and Plasmid-Free Model in the Unstirred Chemostat, *SIAM J. Math. Anal.*, Vol. 38, No. 6, 2007, pp. 1860–1885.